

The Euclidean distribution of Fast Radio Bursts

Niels Oppermann,^{1,2*} Liam D. Connor,^{1,2,3} Ue-Li Pen^{1,2,4,5}

¹Canadian Institute for Theoretical Astrophysics, University of Toronto, 60 St. George Street, Toronto ON, M5S 3H8, Canada

²Dunlap Institute for Astronomy and Astrophysics, University of Toronto, 50 St. George Street, Toronto ON, M5S 3H4, Canada

³Department of Astronomy and Astrophysics, University of Toronto, 50 St. George Street, Toronto ON, M5S 3H4, Canada

⁴Canadian Institute for Advanced Research, 180 Dundas St. West, Toronto ON, M5G 1Z8, Canada

⁵Perimeter Institute for Theoretical Physics, 31 Caroline St. North, Waterloo ON, N2L 2Y5, Canada

Accepted XXX. Received YYY; in original form ZZZ

ABSTRACT

We investigate whether current data on the distribution of observed flux densities of Fast Radio Bursts (FRBs) are consistent with a constant source density in Euclidean space. We use the number of FRBs detected in two surveys with different characteristics along with the observed signal-to-noise ratios of the detected FRBs in a formalism similar to a V/V_{\max} -test to constrain the distribution of flux densities. We find consistency between the data and a Euclidean distribution. Any extension of this model is therefore not data-driven and needs to be motivated separately. As a byproduct we also obtain new improved limits for the FRB rate at 1.4 GHz, which had not been constrained in this way before.

Key words: methods: statistical – pulsars: general

1 INTRODUCTION

Fast Radio Bursts (FRBs) are bright, short radio pulses that are highly dispersed. Most FRBs observed so far have dispersion measures that are much larger than what is expected due to the Milky Way’s interstellar medium. Thus, it is likely that the sources producing these bursts are extragalactic. If most of the dispersion is due to the ionised intergalactic medium, the sources have to be at redshifts of the order of one (e.g., [Champion et al. 2015](#)). In this case, they may soon become useful as cosmological probes (e.g., [Masui & Sigurdson 2015](#)). However, the large observed dispersion may also be due to dense material surrounding the source (e.g., [Connor et al. 2016c](#)), putting them at potentially much smaller distances.

An observable distinction between cosmological models and more local models for the FRB population is given by the distribution of flux densities. This is independent of the pulse dispersion. The simplest model is one in which FRBs are uniformly distributed and their location does not influence any of their observable properties other than that farther bursts appear dimmer. In Euclidean space this leads to an unambiguous prediction for their flux densities, namely

$$dN \propto S^{-(\alpha+1)} dS \quad (1)$$

with $\alpha = 3/2$, where S is the flux density and dN is the number of FRBs with a flux density in an infinitesimal interval

dS . This relation holds independently from their intrinsic luminosity distribution and does not require them to be standard candles. Deviations from an index $3/2$ are for example expected if the number density of FRBs is not constant and/or if their distances are large enough that deviations from Euclidean geometry become important. If FRBs are extragalactic, but local, then the default expectation should be $\alpha = 3/2$. It is worth noting that a constant-density Euclidean distribution is the only model that leads to a clear prediction for the observed flux densities. If FRBs are at large enough distances that the expansion history of the Universe is important, then the population of FRBs can be expected to also have undergone some evolution, thus introducing functional degrees of freedom that are at present completely unconstrained. An additional effect that can in principle influence the measured distribution of flux densities is dispersion smearing, i.e., the dispersion of the pulses’ arrival times within a frequency bin of a survey, resulting in a reduction of the signal-to-noise ratio for very high dispersion measures. If dispersion measures were correlated with distance, this could potentially lead to a systematic flattening of the distribution, but will not affect its shape if the dispersion measure and distance of an FRB are uncorrelated.

In this note we investigate whether the constant-density Euclidean model is consistent with current observations. We do this by studying the one-parametric class of models in which α is a free parameter and which includes the constant-density Euclidean model as a special case. Deriving the observational constraints on the parameter α has the potential of showing that $\alpha = 3/2$ is disfavoured by the data without

* E-mail: niels@cita.utoronto.ca (NO)

the need to make any more complicated model assumptions. We derive constraints from a combination of source counts of different surveys and the observed V/V_{\max} -values (Schmidt 1968).

In the simple constant-density Euclidean model, the power-law behaviour of Eq. (1) is not only valid for the flux densities, but also for any other observable that depends linearly on flux density. One example would be the fluence

$$F = \int dt S(t) \\ = S \tau, \quad (2)$$

where τ is the duration of a burst and S is the average flux density within the interval of length τ . Another example is the observed signal-to-noise ratio, which depends on the flux density of the burst, its duration, and of course on properties of the telescope and the survey. In many cases it can be approximated as

$$s \approx K S \tau^{1/2}, \quad (3)$$

where we include all instrumental properties in the constant K (e.g., Caleb et al. 2016). The detection of an FRB is always subject to a sensitivity cutoff in signal-to-noise, and not in flux density or fluence. This makes the statistics of flux density and fluence more complicated than the statistics of the signal-to-noise ratio s and we choose to cast all equations in terms of s . Note that, as is common in the field, we use the term signal-to-noise ratio to mean the amplitude of the FRB signal plus noise, divided by the standard deviation of the noise, which can be approximately determined empirically for each search window length τ .

We derive the necessary statistical methodology in the following section, discuss the data that we use and show our results in Sect. 3. We conclude with a discussion in Sect. 4.

2 METHODOLOGY

2.1 Likelihood for the observed signal-to-noise ratios

Clearly some information on the parameter α is contained in the distribution of observed signal-to-noise ratios. If we assume a value for α and suppose that a survey with a given signal-to-noise threshold s_{\min} detects an FRB, then the likelihood for its signal-to-noise ratio to be s is, according to Eq. (1),

$$\mathcal{P}(s|s_{\min}, \alpha) = \begin{cases} \frac{\alpha}{s_{\min}} \left(\frac{s}{s_{\min}}\right)^{-(\alpha+1)} & \text{if } s \geq s_{\min} \\ 0 & \text{else} \end{cases}. \quad (4)$$

If the survey detects n independent FRBs then the joint likelihood for their signal-to-noise ratios is simply the product of the individual ones.

For N different surveys, each detecting n_1, \dots, n_N FRBs, the situation is the same, except that we have to take into account that each survey has a different detection threshold s_{\min} . If we denote the observed signal-to-noise value of the i -th FRB in the I -th survey as $s_{I,i}$, the $(n_1 + \dots + n_N)$ -dimensional vector of all these observed values as \vec{s} , the N -dimensional vector of all threshold signal-to-noise values as \vec{s}_{\min} , and the N -dimensional vector of the

numbers of detections in each survey as \vec{n} , the complete likelihood becomes

$$\mathcal{P}(\vec{s}|\vec{n}, \vec{s}_{\min}, \alpha) = \prod_{I=1}^N \prod_{i=1}^{n_I} \mathcal{P}(s_{I,i}|s_{\min,I}, \alpha). \quad (5)$$

This is easily calculated and we will do so in Sect. 3. In the following we will refrain from mentioning \vec{s}_{\min} explicitly in the notation of probabilities and imply that all survey properties are always fixed.

Note that the combination $(s/s_{\min})^{-\alpha}$ for $\alpha = 3/2$ corresponds to the ratio of the volume interior to the FRB and the volume in which this particular FRB could have been detected by the survey, V/V_{\max} , for a constant source density in three-dimensional Euclidean space. The likelihood we are using here to constrain α is thus closely related to the V/V_{\max} -test used in many contexts to check for deviations from a constant density for a source population (e.g., Schmidt 1968).

2.2 Likelihood for the number of observed FRBs

In addition to the information contained in the signal-to-noise ratios of the observed bursts, some information is also contained in the numbers of bursts detected by different surveys. For any one survey, the number of detected FRBs puts constraints on the rate of FRBs occurring above the detection threshold of that survey. This rate can be rescaled to a different survey with a different detection threshold and confronted with the observed number of bursts for that survey. However, the rescaling depends on the parameter α and thus the number of bursts detected by two or more surveys puts constraints on α .

To include these constraints in our analysis we introduce the FRB rate explicitly as an unknown parameter. Since the rate observable by a given survey depends on various properties of the survey, we define the rate r_0 occurring above the detection threshold of a hypothetical survey described by a system temperature $T_{\text{sys},0} = 1$ K, a gain $G_0 = 1$ K Jy $^{-1}$, $n_{\text{p},0} = 2$ observed polarizations, a bandwidth $B_0 = 1$ MHz, and a signal-to-noise threshold $s_{\min,0} = 1$. As explained by Connor et al. (2016a), the FRB rate above the detection threshold of the I -th survey is then a rescaled version of this rate, namely

$$r_I = r_0 \left(\frac{T_{\text{sys},I}}{T_{\text{sys},0}} \frac{G_0}{G_I} \sqrt{\frac{n_{\text{p},0} B_0}{n_{\text{p},I} B_I} \frac{s_{\min,I}}{s_{\min,0}}} \right)^{-\alpha} \\ = r_0 \left(\frac{T_{\text{sys},I}}{G_I} \sqrt{\frac{2 \text{ MHz}}{n_{\text{p},I} B_I} s_{\min,I} \text{ Jy}} \right)^{-\alpha}. \quad (6)$$

The expected number of FRBs detected by the I -th survey will then be

$$M_I = r_I \Omega_I T_I, \quad (7)$$

where Ω_I is the angular size of the survey's field of view and T_I is the time spent surveying. The likelihood for the actual number of FRBs observed in this survey is then a Poissonian distribution with this expectation value,

$$P(n_I|r_0, \alpha) = \frac{M_I^{n_I}}{n_I!} e^{-M_I}. \quad (8)$$

For N surveys the complete likelihood again becomes a product of the likelihoods for the individual surveys,

$$P(\vec{n}|r_0, \alpha) = \prod_{I=1}^N P(n_I|r_0, \alpha), \quad (9)$$

and can be used to put constraints on the distribution of flux densities via the parameter α , as well as on the overall rate of FRBs, here parameterized as the rate above the detection threshold of our hypothetical survey, r_0 .

2.3 Posterior

To get the complete set of constraints on the distribution of flux densities, both from the observed signal-to-noise ratios and from the detection numbers of different surveys, we combine the results of Sects. 2.1 and 2.2. We write the joint likelihood for the number of observed FRBs and their signal-to-noise ratios as

$$\begin{aligned} \mathcal{P}(\vec{s}, \vec{n}|r_0, \alpha) &= \mathcal{P}(\vec{s}|\vec{n}, r_0, \alpha) P(\vec{n}|r_0, \alpha) \\ &= \mathcal{P}(\vec{s}|\vec{n}, \alpha) P(\vec{n}|r_0, \alpha). \end{aligned} \quad (10)$$

If we assume flat priors for r_0 and for $\alpha > 0$, this likelihood is proportional to the joint posterior for the parameter α and the rate r_0 .

The likelihood for observed fluxes within a survey obviously only gives us constraints if the survey has in fact detected at least one FRB. Note, however, that we can in principle include surveys without FRB detection by setting

$$\mathcal{P}(\vec{s}|n = 0, s_{\min}, \alpha) = 1 \quad (11)$$

and thus still use them to constrain the parameter α via their implications on the FRB rate above their detection thresholds. Similarly, the numbers of FRBs detected by different surveys only have implications for the parameter α if we assume that the surveys observe the same source population, described by the same rate r_0 . This assumption will in general be violated if different surveys have different frequency coverage or different observational strategies. Specifically, the observations of a deep and narrow survey will in general not be described by the same statistics as those of a shallow and wide survey, as explained by Connor et al. (2016b). Care is thus warranted when comparing detection numbers of qualitatively different surveys. Such an attempt will require more parameters or simply setting

$$P(n|r_0, \alpha) = 1 \quad (12)$$

for all surveys that are not expected to be described by r_0 .

3 DATA AND RESULTS

We make use of 15 observed FRBs from seven surveys. For definiteness, we list all values used in our calculation in Tables 1 and 2. For the likelihood of the numbers of detected FRBs, we only make use of two dedicated pulsar surveys with well-defined characteristics, namely the High Time Resolution Universe Pulsar Survey (HTRU; Keith et al. 2010) at the Parkes telescope and the Pulsar ALFA survey (PALFA; Cordes et al. 2006) at the Arecibo Observatory. We choose these two surveys because for most other discovered FRBs it is hard to estimate the surveying period T that has been

searched for FRBs, especially in the case of non-detections. The survey of Masui et al. (2015) is similarly well-defined, but sensitive to different frequencies. We assume our parameter r_0 to describe the rate at frequencies around 1.4 GHz and do not want to make any assumption about the relation between this rate and the rate at 800 MHz, which is the central frequency of Masui et al. (2015).

Even for HTRU and PALFA, the parameters needed in Eq. (6) are defined somewhat ambiguously. To avoid building complicated models of the telescopes and surveys, we generally opt for simple choices that can be made consistently for both surveys. Specifically, this means that we do not include any estimate of the sky temperature due to the Milky Way in the values we assume for the system temperature T_{sys} . For the gain G we use the arithmetic mean of the gains corresponding to the beam centres of the multibeam receivers. The bandwidth B does not include frequencies deemed unusable by the surveying team and the angular size of the field of view Ω is intended to approximate the area within the half-maximum beam power. The resulting numerical values are listed in Table 1. Other reasonable choices for these parameters will typically lead to deviations on the order of 10%. Note that the exact definition of each parameter does not impact the results as long as the same definition is used for all surveys that are being compared.

For the constraint on α coming from the likelihood for the observed signal-to-noise ratios, we can use all detected FRBs, as long as there is a well-defined signal-to-noise cutoff s_{\min} . Since we are investigating the population of sources, we are not including repeated bursts from the same object (Spitler et al. 2016). We also exclude the single burst detections by Lorimer et al. (2007) and Keane et al. (2011), since no definitive value of s_{\min} can be determined. We list the values of s and s_{\min} that we use in Table 2.

After calculating the two-dimensional posterior for α and r_0 , we derive the final constraint on α by marginalising over r_0 and vice versa. These posterior distributions are shown in Fig. 1.

4 DISCUSSION

Figure 1 shows a strong correlation between the FRB rate and the slope parameter α . This can be understood in terms of regions of parameter space that are in tension with the data. If the rate of FRBs is high, a shallow flux density distribution will overpredict the number of FRBs occurring at high signal-to-noise ratios. If the rate is low, on the other hand, a steep distribution will underpredict the number of FRBs occurring above the detection threshold of current surveys, especially at high signal-to-noise values.

The figure also shows the posterior distributions that are obtained if only the detection numbers or the signal-to-noise ratios are used, instead of their combination. Obviously, the signal-to-noise ratios alone do not constrain the FRB rate at all. Thus, the corresponding contours appear as horizontal lines in the main panel of the figure. And even for the parameter α , the main constraint comes from the comparison of the detection numbers for the two surveys HTRU and PALFA. Using the signal-to-noise ratios in addition does, however, add some information, in that it rules out close-to-flat flux distributions and very low rates.

Table 1. Parameters assumed for the FRB surveys. See Sect. 2.2 for the meaning of the symbols.

survey ¹	s_{\min}	T_{sys}/K	$G/(\text{K}/\text{Jy})$	n_{p}	B/MHz	$\Omega/(\text{deg}^2)$	T/h	n
HTRU [1]	10	23	0.64	2	340	13×0.043	3650	9
PALFA [2]	7	30	8.5	2	300	7×0.0027	886	1

¹ [1] Champion et al. 2015; Thornton et al. 2013; Keith et al. 2010; [2] Spitler et al. 2014; Cordes et al. 2006

Table 2. Parameters of each individual FRB used in our calculation. The signal-to-noise ratios s are taken from the FRBcat website¹ (Petroff et al. 2016).

name	s	s_{\min}	survey ²
FRB090625	30	10	[1]
FRB110220	49	10	[1]
FRB110626	11	10	[1]
FRB110703	16	10	[1]
FRB120127	11	10	[1]
FRB121002	16	10	[1]
FRB130626	21	10	[1]
FRB130628	29	10	[1]
FRB130729	14	10	[1]
FRB121102	14	7	[2]
FRB010125	17	7	[3]
FRB131104	30	8	[4]
FRB140514	16	10	[5]
FRB150418	39	10	[6]
FRB110523	42	8	[7]

¹ <http://www.astronomy.swin.edu.au/pulsar/frbcat/>

² [1] Champion et al. 2015; Thornton et al. 2013; Keith et al. 2010; [2] Spitler et al. 2014; Scholz et al. 2016; [3] Burke-Spolaor & Bannister 2014; [4] Ravi et al. 2015; [5] Petroff et al. 2015; [6] Keane et al. 2016; [7] Masui et al. 2015; Connor et al. 2016a

The full posterior for the parameter α still allows a wide range of values. The 95% confidence interval is

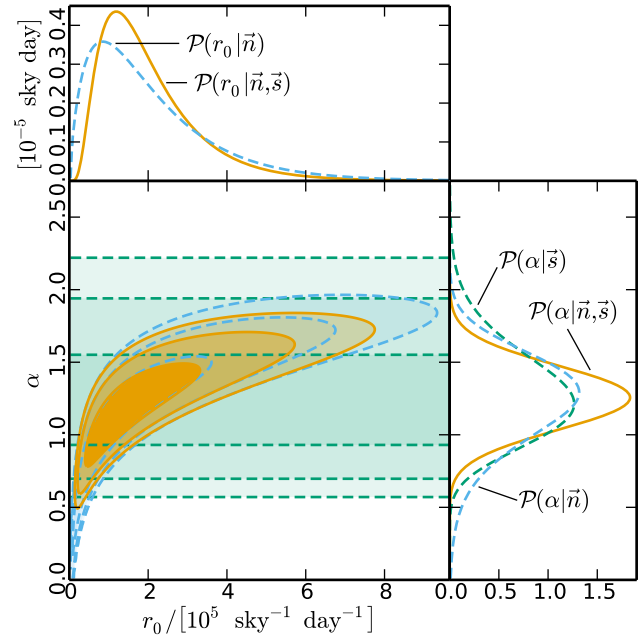
$$0.8 \leq \alpha \leq 1.7. \quad (13)$$

This is to be contrasted with recent results from the literature. Caleb et al. (2016), for example, find $\alpha = 0.9 \pm 0.3$ and Li et al. (2016) claim $\alpha = 0.14 \pm 0.20$. We stress that our constraints are model-independent in the sense that we have not assumed any specific relation between flux density, burst duration, and dispersion measure. An important conclusion of our analysis is that the simplest possible model for the distribution of FRBs, constant density in Euclidean space, is consistent with current data. Of course this does not mean that it is proven to be correct, but it does mean that any extension to this model is not data-driven but has to be motivated independently. This finding is consistent with the qualitative conclusions of Katz (2016b) and Katz (2016a).

As a byproduct of our attempt to constrain α , we also obtain constraints on the rate of FRBs at 1.4 GHz. The 95% confidence interval for our parameter r_0 is

$$4.8 \times 10^4 \text{ sky}^{-1} \text{ day}^{-1} \leq r_0 \leq 5.3 \times 10^5 \text{ sky}^{-1} \text{ day}^{-1}. \quad (14)$$

It may be worth noting that the constraints on the FRB rate tighten up somewhat if the parameter α is fixed. In

**Figure 1.** Posterior distribution for the parameter α describing the distribution of FRB flux densities and the FRB rate r_0 . The bottom left panel shows the two-dimensional posterior for both parameters, the smaller panels show the marginalised posteriors for each parameter individually. We show separate curves and contours for the constraints coming from the signal-to-noise ratios \vec{s} (green dashed), from the detection numbers \vec{n} (blue dashed), and their combination (orange solid). The contour lines show the 68%, 95%, and 99% confidence regions.

the constant-density Euclidean model, for example, the 95% confidence limit on the rate is

$$1.6 \times 10^5 \text{ sky}^{-1} \text{ day}^{-1} \leq r_{0,\alpha=3/2} \leq 5.4 \times 10^5 \text{ sky}^{-1} \text{ day}^{-1}. \quad (15)$$

For any specific survey this rate has to be rescaled according to Eq. (6). As an example we calculate the FRB rate above the detection threshold of the HTRU survey, again for $\alpha = 3/2$,

$$1.9 \times 10^3 \text{ sky}^{-1} \text{ day}^{-1} \leq r_{\text{HTRU},\alpha=3/2} \leq 6.3 \times 10^3 \text{ sky}^{-1} \text{ day}^{-1}. \quad (16)$$

These are slightly lower values than the range derived by Champion et al. (2015). We stress again that all rates we calculate are subject to a signal-to-noise cutoff. Converting

them to rates above a given fluence is impossible without making further assumptions.

ACKNOWLEDGEMENTS

We thank Vikram Ravi and Kiyo Masui for helpful discussions and Jonathan Katz, Evan Keane, and an anonymous referee for useful comments on the manuscript. This research has made use of NASA’s Astrophysics Data System. The figure was produced using the `matplotlib` library (Hunter 2007) and we acknowledge use of the FRBCAT database (Petroff et al. 2016). We acknowledge NSERC support.

REFERENCES

- Burke-Spolaor, S. & Bannister, K. W., The Galactic Position Dependence of Fast Radio Bursts and the Discovery of FRB011025, *ApJ* **792** (Sep. 2014) 19, [arXiv:1407.0400 \[astro-ph.HE\]](#)
- Caleb, M., Flynn, C., Bailes, M., et al., Are the distributions of fast radio burst properties consistent with a cosmological population?, *MNRAS* **458** (May 2016) 708–717, [arXiv:1512.02738 \[astro-ph.HE\]](#)
- Champion, D. J., Petroff, E., Kramer, M., et al., Five new Fast Radio Bursts from the HTRU high latitude survey: first evidence for two-component bursts, ArXiv e-prints (Nov. 2015), [arXiv:1511.07746 \[astro-ph.HE\]](#)
- Connor, L., Lin, H.-H., Masui, K., et al., Constraints on the FRB rate at 700-900 MHz, ArXiv e-prints (Feb. 2016), [arXiv:1602.07292 \[astro-ph.HE\]](#)
- Connor, L., Pen, U.-L., & Oppermann, N., FRB repetition and non-Poissonian statistics, *MNRAS* **458** (May 2016) L89–L93, [arXiv:1601.04051 \[astro-ph.HE\]](#)
- Connor, L., Sievers, J., & Pen, U.-L., Non-cosmological FRBs from young supernova remnant pulsars, *MNRAS* **458** (May 2016) L19–L23, [arXiv:1505.05535 \[astro-ph.HE\]](#)
- Cordes, J. M., Freire, P. C. C., Lorimer, D. R., et al., Arecibo Pulsar Survey Using ALFA. I. Survey Strategy and First Discoveries, *ApJ* **637** (Jan. 2006) 446–455, [astro-ph/0509732](#)
- Hunter, J. D., Matplotlib: A 2D graphics environment, *Computing In Science & Engineering* **9** no. 3, (2007) 90–95
- Katz, J. I., Fast radio bursts — A brief review: Some questions, fewer answers, *Modern Physics Letters A* **31** (Apr. 2016) 1630013, [arXiv:1604.01799 \[astro-ph.HE\]](#)
- Katz, J. I., Inferences from the Distributions of Fast Radio Burst Pulse Widths, Dispersion Measures, and Fluences, *ApJ* **818** (Feb. 2016) 19, [arXiv:1505.06220 \[astro-ph.HE\]](#)
- Keane, E. F., Johnston, S., Bhandari, S., et al., The host galaxy of a fast radio burst, *Nature* **530** (Feb. 2016) 453–456, [arXiv:1602.07477 \[astro-ph.HE\]](#)
- Keane, E. F., Kramer, M., Lyne, A. G., Stappers, B. W., & McLaughlin, M. A., Rotating Radio Transients: new discoveries, timing solutions and musings, *MNRAS* **415** (Aug. 2011) 3065–3080, [arXiv:1104.2727 \[astro-ph.SR\]](#)
- Keith, M. J., Jameson, A., van Straten, W., et al., The High Time Resolution Universe Pulsar Survey - I. System configuration and initial discoveries, *MNRAS* **409** (Dec. 2010) 619–627, [arXiv:1006.5744 \[astro-ph.HE\]](#)
- Li, L., Huang, Y., Zhang, Z., Li, D., & Li, B., Intensity Distribution Function and Statistical Properties of Fast Radio Bursts, ArXiv e-prints (Feb. 2016), [arXiv:1602.06099 \[astro-ph.HE\]](#)
- Lorimer, D. R., Bailes, M., McLaughlin, M. A., Narkevic, D. J., & Crawford, F., A Bright Millisecond Radio Burst of Extragalactic Origin, *Science* **318** (Nov. 2007) 777, [arXiv:0709.4301](#)
- Masui, K., Lin, H.-H., Sievers, J., et al., Dense magnetized plasma associated with a fast radio burst, *Nature* **528** (Dec. 2015) 523–525, [arXiv:1512.00529 \[astro-ph.HE\]](#)
- Masui, K. W. & Sigurdson, K., Dispersion Distance and the Matter Distribution of the Universe in Dispersion Space, *Physical Review Letters* **115** no. 12, (Sep. 2015) 121301, [arXiv:1506.01704](#)
- Petroff, E., Bailes, M., Barr, E. D., et al., A real-time fast radio burst: polarization detection and multiwavelength follow-up, *MNRAS* **447** (Feb. 2015) 246–255, [arXiv:1412.0342 \[astro-ph.HE\]](#)
- Petroff, E., Barr, E. D., Jameson, A., et al., FRBCAT: The Fast Radio Burst Catalogue, ArXiv e-prints (Jan. 2016), [arXiv:1601.03547 \[astro-ph.HE\]](#)
- Ravi, V., Shannon, R. M., & Jameson, A., A Fast Radio Burst in the Direction of the Carina Dwarf Spheroidal Galaxy, *ApJ* **799** (Jan. 2015) L5, [arXiv:1412.1599 \[astro-ph.HE\]](#)
- Schmidt, M., Space Distribution and Luminosity Functions of Quasi-Stellar Radio Sources, *ApJ* **151** (Feb. 1968) 393
- Scholz, P., Spitler, L. G., Hessels, J. W. T., et al., The repeating Fast Radio Burst FRB 121102: Multi-wavelength observations and additional bursts, ArXiv e-prints (Mar. 2016), [arXiv:1603.08880 \[astro-ph.HE\]](#)
- Spitler, L. G., Cordes, J. M., Hessels, J. W. T., et al., Fast Radio Burst Discovered in the Arecibo Pulsar ALFA Survey, *ApJ* **790** (Aug. 2014) 101, [arXiv:1404.2934 \[astro-ph.HE\]](#)
- Spitler, L. G., Scholz, P., Hessels, J. W. T., et al., A repeating fast radio burst, *Nature* **531** (Mar. 2016) 202–205, [arXiv:1603.00581 \[astro-ph.HE\]](#)
- Thornton, D., Stappers, B., Bailes, M., et al., A Population of Fast Radio Bursts at Cosmological Distances, *Science* **341** (Jul. 2013) 53–56, [arXiv:1307.1628 \[astro-ph.HE\]](#)

This paper has been typeset from a $\text{\TeX}/\text{\LaTeX}$ file prepared by the author.